

Long non-coding RNA DDX11-AS1 promotes the proliferation and migration of glioma cells by combining with HNRNPC

Zijin Xiang,¹ Qiaoli Lv,² Yujun Zhang,¹ Xueru Chen,¹ Ren Guo,¹ Shikun Liu,¹ and Xiangdong Peng¹

¹Department of Pharmacy, The Third Xiangya Hospital, Central South University, Changsha 410013, Hunan, China; ²Jiangxi Key Laboratory of Translational Cancer Research, Department of Head and Neck Surgery, Jiangxi Cancer Hospital of Nanchang University, Nanchang, China

Glioma is a malignant tumor of the central nervous system with complex pathogenesis, difficult operation, and a high postoperative recurrence rate. At present, there is still a lack of effective treatment. Long non-coding RNA DDX11 antisense RNA 1 (DDX11-AS1) has been shown to promote tumor development, such as hepatocellular carcinoma, esophageal cancer, etc. However, its molecular mechanism in glioma is poorly understood. In this study, we found that the expression of DDX11-AS1 was elevated in glioma tissues, and patients with high expression of DDX11-AS1 had poor prognosis. DDX11-AS1 was a potential prognostic marker. Functionally, DDX11-AS1 promoted glioma cell proliferation and migration. Mechanistically, DDX11-AS1 interacted with RNA-binding protein heterogeneous nuclear ribonucleoprotein C (HNRNPC) to promote Wnt/ β -catenin and AKT pathways and the epithelial-mesenchymal transition process. In summary, our study manifests that the DDX11-AS1/HNRNPC axis may play a vital part in the occurrence and development of glioma, which provides new ideas and therapeutic targets for the diagnosis, treatment, and prognosis of glioma.

INTRODUCTION

Glioma is one of the refractory malignant tumors worldwide, with characteristics including a high recurrence rate and poor clinical prognosis.^{1,2} More than 50% of malignant tumors of the central nervous system are gliomas.³ The etiology of glioma is unclear, and its potential causes may include genetic diseases, environmental carcinogens, viral infections, dietary factors, etc. However, these factors often lead to changes in the tumor microenvironment, signaling molecules, and other internal factors to promote the occurrence and development of glioma.⁴ Therefore, the study of the genesis and development mechanism of glioma at the genetic and molecular level can provide a new theoretical basis for the diagnosis and treatment of glioma.

Growing studies have shown that long non-coding RNAs (lncRNAs) can regulate the proliferation, metastasis, and angiogenesis of cancer cells.⁵ lncRNAs are also abnormally expressed during cancer development, which directly or indirectly regulates cancer-related signals through various pathways, thus affecting the occur-

rence and development of various tumors, including glioma.⁶ For example, lncRNA CRNDE activates mTOR signaling or attenuates the miR-384/PIWIL4/STAT3 axis to promote glioma cell growth and migration.^{7,8} lncRNA NEAT1 promotes glioblastoma progression through the WNT/ β -catenin pathway and the let-7g-5p/MAP3K1 axis.^{9,10} These results also suggest that lncRNAs can regulate the malignant biological behavior of gliomas by different molecular mechanisms.

Recent researches have reported that lncRNA DDX11 antisense RNA 1 (DDX11-AS1) is involved in the development of hepatocellular carcinoma, esophageal cancer, bladder cancer, non-small cell lung cancer, and other cancers.^{11–19} In general, patients with high expression of DDX11-AS1 generally have a poor prognosis.¹³ DDX11-AS1 acts as an oncogene that increases cancer cell proliferation, migration, or drug resistance by various molecular mechanisms.^{13,14,16,19} However, the role of DDX11-AS1 in glioma and its potential molecular mechanisms are poorly known.

In this study, we comprehensively analyzed the expression of DDX11-AS1 in glioma and its relationship with patient prognosis through The Cancer Genome Atlas (TCGA), Gene Expression Omnibus (GEO), and Chinese Glioma Genome Atlas (CGGA) databases. Further, we detected DDX11-AS1 expression in 26 normal samples and 88 glioma samples. After the construction of knockdown and overexpressed DDX11-AS1 glioma cells, we performed cell-function experiments. We explored the deep mechanism of DDX11-AS1's interaction with RNA-binding protein (RBP) heterogeneous nuclear ribonucleoprotein C (HNRNPC). Generally, we aimed to analyze the role and mechanism of lncRNA DDX11-AS1 in the occurrence and development of glioma through cell experiments and clinical specimen detection and provide a theoretical basis for the diagnosis and treatment of glioma.

Received 16 November 2021; accepted 23 April 2022;
<https://doi.org/10.1016/j.omtn.2022.04.016>

Correspondence: Xiangdong Peng, Department of Pharmacy, The Third Xiangya Hospital of Central South University, 138 Tongzipo Rd. Changsha City, Hunan Province, China 410013.

E-mail: xdpeng@csu.edu.cn



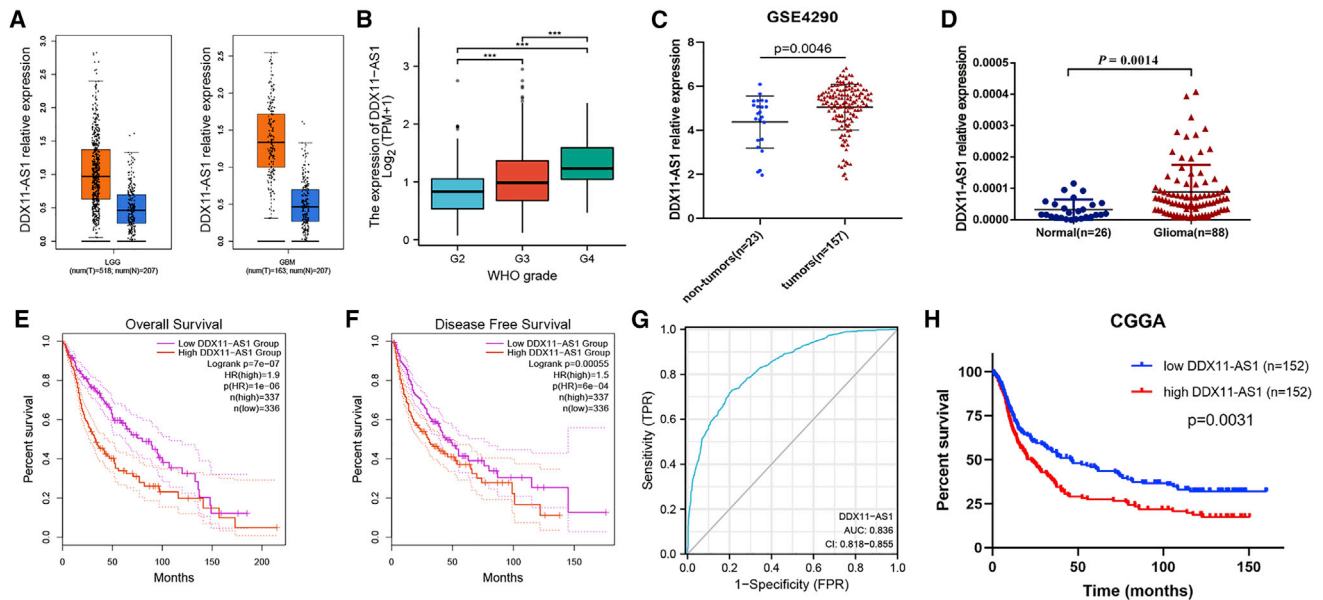


Figure 1. The expression of DDX11-AS1 in glioma and its relationship with prognosis

(A and B) The expression of DDX11-AS1 in TCGA database. *** $p < 0.001$. (C) The expression of DDX11-AS1 in the GSE4290 database. (D) The quantitative real-time PCR detection of DDX11-AS1 expression in 26 normal samples and 88 glioma samples. (E) The Kaplan-Meier curves for survival analysis of DDX11-AS1 from the TCGA database. (F) The Kaplan-Meier curves for disease-free analysis of DDX11-AS1 from the TCGA database. (G) The ROC curve analysis of DDX11-AS1 in TCGA and GTEx databases for predicting outcomes of glioma patients. (AUC = 0.836, CI = 0.818–0.855). (H) The Kaplan-Meier curves for survival analysis of DDX11-AS1 from the CGGA database. Results represent means \pm SEM. $p < 0.05$ was considered statistically significant.

RESULTS

DDX11-AS1 is up-regulated in glioma tissues, and high-expressed DDX11-AS1 is associated with poor prognoses of glioma patients

To explore the expression pattern of DDX11-AS1 in glioma tissues, we conducted an in-depth analysis of TCGA data on the GEPIA website. Since there is no glioma control tissue sample in TCGA data, by matching GTEx data, the expression of DDX11-AS1 in 518 cases of low-grade glioma (LGG) and 163 cases of glioblastoma (GBM) was significantly increased compared with 207 normal samples (Figure 1A). With the increase of grade, the expression level also gradually increased (Figure 1B). We found that DDX11-AS1 was also highly expressed in glioma tissues after data analysis of the GSE4290 dataset (Figure 1C). Furthermore, we collected 26 normal samples and 88 gliomas for DDX11-AS1 quantitative analysis by quantitative real-time PCR, and the results were consistent with the database analysis (Figure 1D). After evenly distributing all glioma samples according to DDX11-AS1 expression levels, we found that the overall survival and disease-free survival rates were higher in the group with low DDX11-AS1 expression, especially within 5 years (120 months) (Figures 1E and 1F). The receiver operating characteristic curve (ROC curve) based on TCGA and GTEx glioma data showed that DDX11-AS1 had a high accuracy in predicting the outcome of glioma patients (area under the curve [AUC] = 0.836, confidence interval [CI] = 0.818–0.855) (Figure 1G). By analyzing the CGGA database, we also found that patients with low expression of DDX11-AS1 had a better prognosis (Figure 1H). Moreover, based on the baseline clin-

ical data of these patients in TCGA and CGGA databases, we observed that tumor stage, age, isocitrate dehydrogenase (IDH) mutation status, and 1p19q code status were correlated with the expression of DDX11-AS1 (Tables 1 and 2). These results indicated that DDX11-AS1 was related to the progression of glioma.

DDX11-AS1 promotes glioma cell migration and the epithelial-mesenchymal transition (EMT) process

Next, we constructed knockdown and overexpressed DDX11-AS1 cell models for cell-function experiments (Figure S1). Through transwell and wound-healing assays, we observed that the migration ability of glioma cells with low-expressed DDX11-AS1 was weakened, while the migration ability of glioma cells with high expression was enhanced (Figures 2A and 2B). EMT is a biological process in which epithelial cells are transformed into mesenchymal cells through specific procedures. It is reported that the adhesion ability of tumor cells activated by EMT is significantly weakened, which facilitates cell migration and triggers tumor metastasis. In the process of EMT, epithelial cell adhesion molecule E-cadherin decreases, and mesenchymal proteins such as N-cadherin and vimentin increase.^{20–22} We proceeded to detect the protein expression of E-cadherin, N-cadherin, and vimentin. The results showed that the expression of E-cadherin was increased and that the expression of N-cadherin and vimentin were decreased in DDX11-AS1 knockdown cells (Figure 2C). This implied that DDX11-AS1 knockdown inhibited the EMT process; in contrast, DDX11-AS1 overexpression activated the EMT process (Figure 2D).

Table 1. Correlation between DDX11-AS1 expression and clinical features of glioma in TCGA

Characteristic	Low expression of DDX11-AS1	High expression of DDX11-AS1	p
Total	348	348	
WHO grade, n (%)			<0.001
G2	156 (24.6)	68 (10.7)	
G3	127 (20)	116 (18.3)	
G4	33 (5.2)	135 (21.3)	
IDH.mutation. status, n (%)			<0.001
WT	86 (12.5)	160 (23.3)	
Mut	257 (37.5)	183 (26.7)	
1p19q.codel. status, n (%)			0.001
codel	67 (9.7)	104 (15.1)	
non-codel	280 (40.6)	238 (34.5)	
Age, median (IQR)	41 (31, 54)	51 (37.75, 60)	<0.001

WT, wild-type; Mut, mutant; IQR, interquartile range.

DDX11-AS1 increases the proliferation ability of glioma cells *in vivo* and *in vitro*

To investigate the effect of DDX11-AS1 on cell proliferation, we conducted experiments *in vivo* and *in vitro*. The results of the MTT assay showed that the proliferation ability of T98G and HS683 cells decreased after knocking down DDX11-AS1 (Figure 3A). The colony formation of cells with DDX11-AS1 knockdown was significantly reduced, and the colony formation of cells with high DDX11-AS1 expression increased (Figure 3B). Furthermore, flow-cytometry analysis of apoptosis showed that the number of glioma cells with low expression of DDX11-AS1 increased (Figure 3C). In addition, we conducted tumor-formation experiments *in vivo*. We subcutaneously inoculated HS683 cells with DDX11-AS1 overexpression in the armpits of nude mice. The tumor growth is shown in Figure 3D. The growth of DDX11-AS1 overexpressed cells was faster. In addition, immunohistochemical (IHC) results showed that Ki67 expression levels increased in the overexpression group (Figure 3E). Since the Wnt/ β -catenin and AKT pathways are closely related to the occurrence and development of glioma,^{23,24} we also observed that DDX11-AS1 knockdown inhibited these two pathways, while overexpression activated them, by western blot (Figures 3F and 3G). IHC analysis also showed increased expression of β -catenin in the DDX11-AS1 group (Figure 3E). Therefore, DDX11-AS1 promoted the occurrence and development of glioma.

DDX11-AS1 interacts with HNRNPC

The research reports that DDX11-AS1 is highly expressed in the cytoplasm of glioma cells.²⁵ Moreover, increasing studies have shown that lncRNA regulation of cell function in the cytoplasm depends on proteins.^{26,27} Therefore, to explore the potential binding proteins of DDX11-AS1, we predicted the binding RBPs of DDX11-AS1 on star-Base v.2.0, and the results showed that DDX11-AS1 can bind 43

Table 2. Correlation between DDX11-AS1 expression and clinical features of glioma in CGGA

Characteristic	Low expression of DDX11-AS1	High expression of DDX11-AS1	p
Total	152	152	
PRS.type, n (%)			0.4055
Primary	109 (35.9)	110 (36.2)	
Recurrent	28 (9.2)	30 (9.9)	
Secondary	15 (4.9)	12 (3.9)	
Grade, n (%)			<0.0001
WHO II	75 (24.7)	22 (7.2)	
WHO III	40 (13.2)	33 (10.9)	
WHO IV	37 (12.2)	97 (31.9)	
Gender, n (%)			0.8294
Male	93 (30.6)	96 (31.6)	
Female	59 (19.4)	56 (18.4)	
Age, n (%)			0.0002
>40	66 (21.7)	106 (34.9)	
≤40	86 (28.3)	46 (15.1)	
IDH.mutation. status, n (%)			<0.0001
Mutant	131 (43.1)	32 (10.5)	
Wild type	21 (6.9)	120 (39.5)	
1p19q.codel. status, n (%)			<0.0001
Codel	59 (19.4)	3 (1)	
Non-codel	93 (30.6)	149 (49)	

RBPs. Furthermore, T98G cells were collected for chromatin isolation by RNA purification and mass spectrometry (CHIRP-MS) analysis to identify the proteins bound by DDX11-AS1. Compared with the control (Ctrl) group, DDX11-AS1 specifically binds to 208 proteins. We mainly focused on the top 50 proteins in the iBAQ score. Then, after the two sets of proteins intersected, there were only HNRNPC and PTBP1 (Figure 4A). Because HNRNPC interacted with DDX11-AS1 more abundantly, HNRNPC was listed as a candidate molecule for a subsequent mechanism study. Furthermore, to verify the direct binding of DDX11-AS1 to HNRNPC, we performed RBP immunoprecipitation (RIP) experiments using HNRNPC antibody to pull down the RNA molecules bound by HNRNPC. By quantitative real-time PCR detection and analysis, compared with the immunoglobulin G (IgG) Ctrl group, DDX11-AS1 was significantly enriched by the HNRNPC antibody (Figure 4B). In addition, we analyzed the correlation between the expression of DDX11-AS1 and HNRNPC in the TCGA and CGGA databases. DDX11-AS1 was positively correlated with HNRNPC (Figures 4C and 4D). We also found that HNRNPC was highly expressed in glioma tissues and that patients with low HNRNPC expression had a better prognosis (Figures 4E–4G). By western-blot analysis, the expression of HNRNPC decreased with the knockdown of DDX11-AS1, and the expression of HNRNPC increased with the overexpression of DDX11-AS1 (Figures 4H and

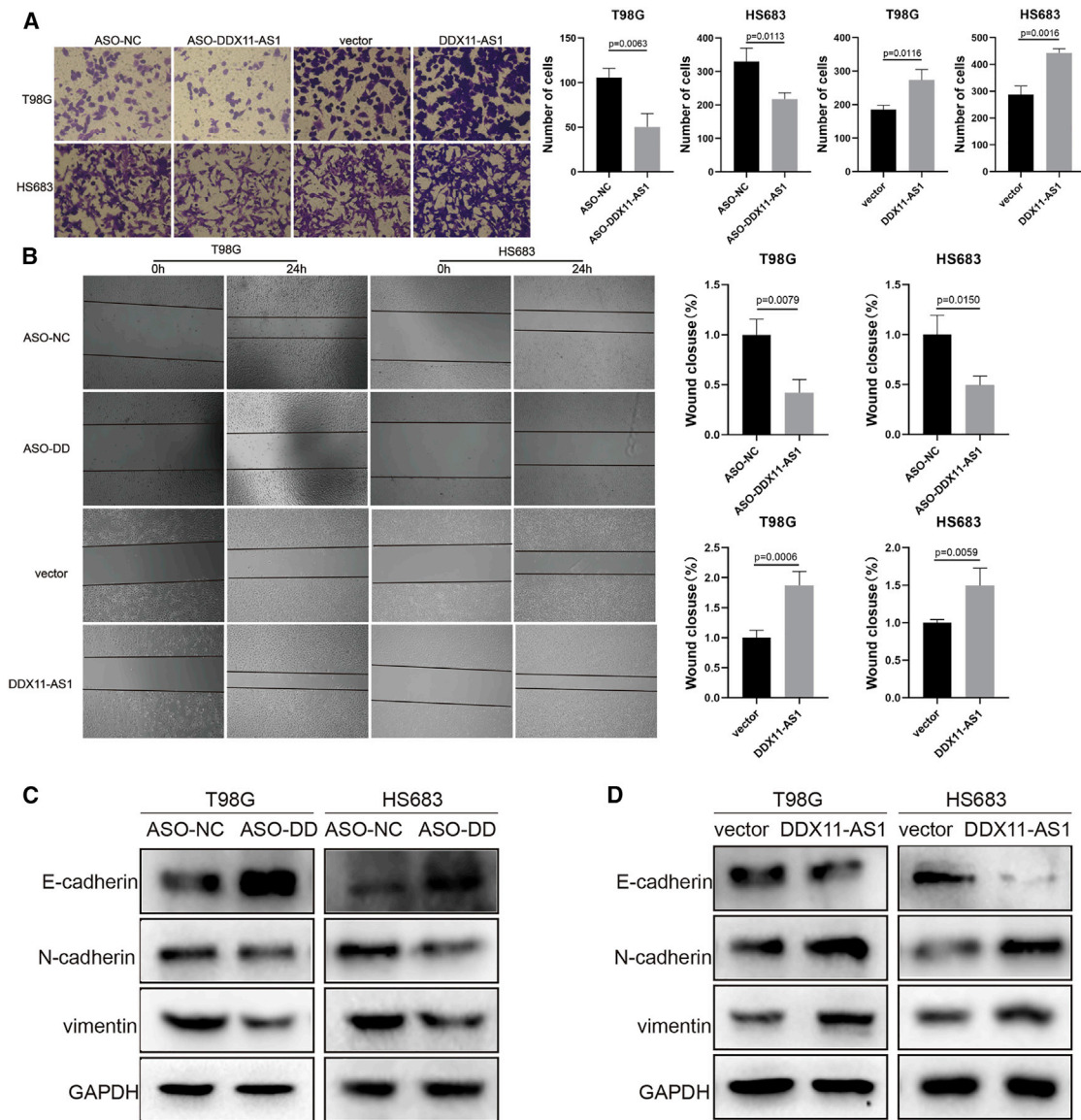


Figure 2. The effect of DDX11-AS1 on glioma cell migration

(A) The transwell experiment of DDX11-AS1 overexpression and knockdown. (B) The wound-healing assay of DDX11-AS1 overexpression and knockdown. (C and D) The western-blot assay of DDX11-AS1 on the EMT process. Results represent means \pm SEM. $n = 3$. $p < 0.05$ was considered statistically significant.

4I). Furthermore, we constructed three small interfering RNAs (siRNAs) for HNRNPC knockdown, and the third sequence was the best knockdown, which was then used in subsequent experiments (Figure 4). In summary, these data indicated that DDX11-AS1 could specifically bind to HNRNPC and that HNRNPC was the target of DDX11-AS1.

HNRNPC knockdown inhibits glioma cell proliferation, migration, and EMT *in vitro*

Next, we explored the functional role of HNRNPC in glioma. After knocking down HNRNPC, the clone-formation experiment showed

that the proliferation ability of glioma cells decreased (Figure 5A), and the wound-healing assay demonstrated that glioma cell migration was reduced (Figure 5B). These results suggested that HNRNPC knockdown inhibited the proliferation and migration of glioma cells. In addition, we also found that HNRNPC affected Wnt/ β -catenin and AKT pathways and the EMT process (Figure 5C).

DDX11-AS1 promotes glioma progression through HNRNPC

We tried to explore whether the effect of DDX11-AS1 on the progression of glioma depended on HNRNPC. Based on the overexpression of DDX11-AS1, we further knocked down HNRNPC to

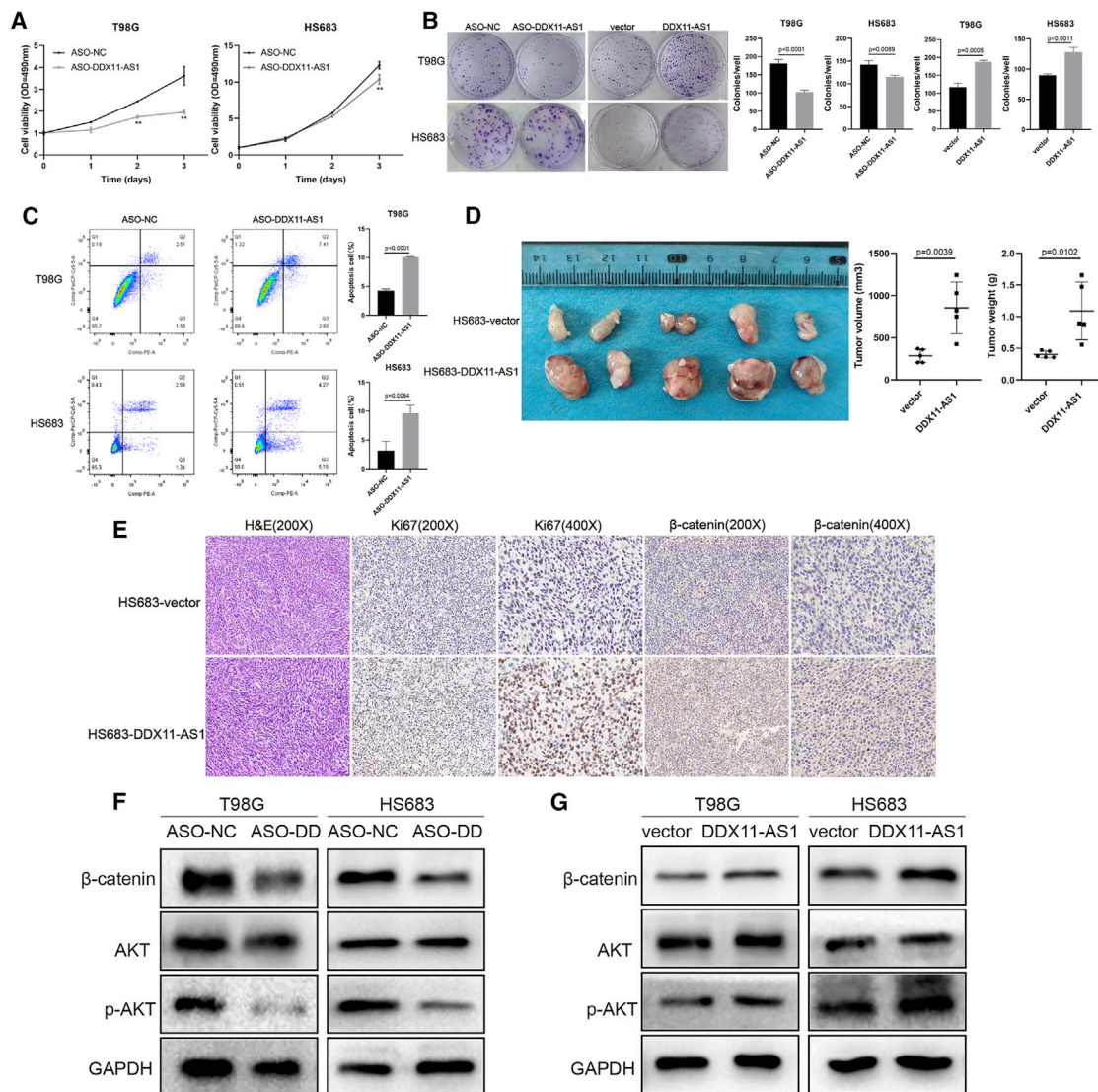


Figure 3. The proliferation effect of DDX11-AS1 on glioma cells *in vivo* and *in vitro*

(A) The MTT assay of DDX11-AS1 knockdown. ** $p < 0.01$. (B) The clone-formation assay of DDX11-AS1 overexpression and knockdown. (C) The cell apoptosis was detected by flow cytometry. (D) Subcutaneous xenograft experiments and volume and weight of tumor growth in overexpressed DDX11-AS1 and control groups. $n = 5$. (E) The immunohistochemical analysis of Ki67 and β -catenin in animal tissue samples. (F and G) The western-blot assay of DDX11-AS1 on the Wnt/ β -catenin and AKT pathways. Results represent means \pm SEM. $p < 0.05$ was considered statistically significant.

perform cell-proliferation and migration experiments. We observed that the ability of DDX11-AS1 to promote the proliferation and migration of glioma cells was attenuated by the knockdown of HNRNPC (Figures 6A and 6B). In addition, we also analyzed the role of the DDX11-AS1/HNRNPC axis *in vivo*. For this, we designed the HNRNPC knockdown lentivirus, the knockdown efficiency of which is shown in Figure S2. Tumorigenesis results in nude mice showed that HNRNPC knockdown attenuated the glioma growth-promoting effect of DDX11-AS1 (Figure 6C). Moreover, western-blot analysis demonstrated that HNRNPC knockdown reduced the activation of Wnt/ β -catenin and AKT pathways

and the EMT process by DDX11-AS1 (Figure 6D). Further, according to the expression of DDX11-AS1 and HNRNPC in CGGA glioma patients, the patients were divided into four groups for overall-survival analysis. As shown in Figure 6E, patients with low expression of both DDX11-AS1 and HNRNPC had the highest survival rate.

DISCUSSION

LncRNAs have regulatory effects on human biological functions and the occurrence and development of diseases and have gradually attracted the attention of researchers in recent years.²⁸ At

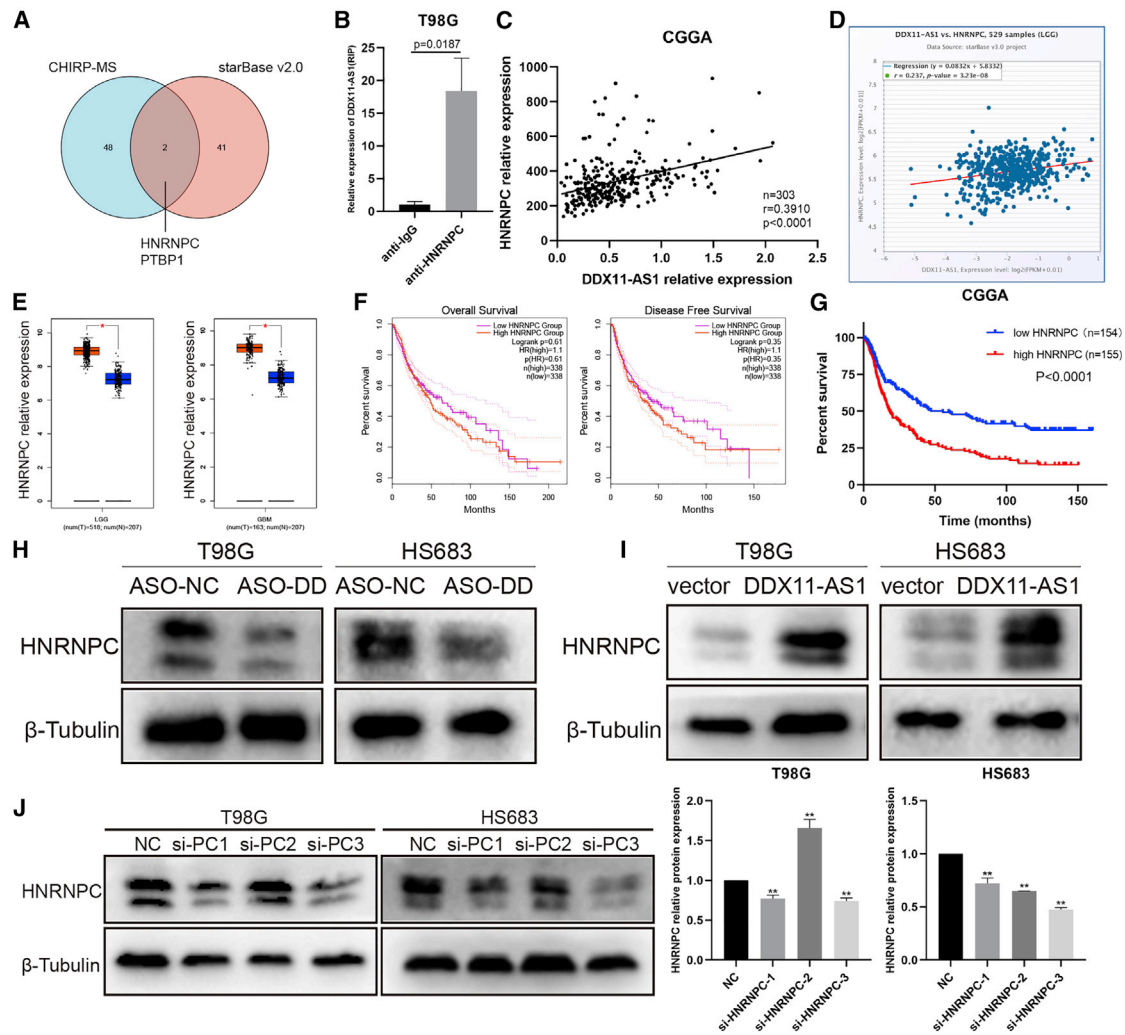


Figure 4. HNRNPC was the direct target of DDX11-AS1

(A) CHIRP-MS and starBase v.2.0 analysis for DDX11-AS1 binding proteins. (B) The expression of DDX11-AS1 combined with anti-HNRNPC antibody and anti-IgG antibody was determined by RIP assay. (C and D) The correlation analysis between DDX11-AS1 and HNRNPC in glioma samples from the CGGA and TCGA databases. (E) The expression of HNRNPC in the TCGA database. (F) The Kaplan-Meier curves for survival analysis and disease-free analysis of HNRNPC from the TCGA database. (G) The Kaplan-Meier curves for survival analysis of HNRNPC from the CGGA database. (H) DDX11-AS1 knockdown inhibited the expression of HNRNPC. (I) Overexpression of DDX11-AS1 increased the expression of HNRNPC. (J) The western blot analysis of HNRNPC knockdown by three different siRNA sequences. Results represent means \pm SEM. $p < 0.05$ was considered statistically significant.

present, tens of thousands of lncRNAs have been identified that are related to gene-regulation imbalance and abnormal biological processes in cancer.²⁹ More importantly, abnormal lncRNAs in clinical specimens have important clinical significance for the diagnosis and prognosis of the tumor. As a novel oncogene, DDX11-AS1 is expected to be a tumor marker or therapeutic target.¹³ In many studies, DDX11-AS1 is mainly involved in the ceRNA regulatory network to promote tumor progression.¹³ Zheng et al. find that the DDX11-AS1/mir-499B-5p/RWDD4 axis promotes the proliferation of glioma cells.²⁵ However, the potential other molecular mechanisms of DDX11-AS1 in glioma are poorly understood.

In our study, we comprehensively analyzed the high expression level of DDX11-AS1 in glioma tissues in multiple databases. Patients with high expression of DDX11-AS1 had lower 5-year overall and disease-free survival. By verifying the functional phenotype in DDX11-AS1 knockdown and overexpression models, we found that DDX11-AS1 promoted glioma cell proliferation and migration and that DDX11-AS1 knockdown also increased the apoptotic ability of glioma cells. In addition, DDX11-AS1 promoted tumor growth *in vivo*. We also discovered that DDX11-AS1 activated the Wnt/ β -catenin and AKT pathways and EMT by western blot. These results suggested that DDX11-AS1 promoted the progression of glioma.

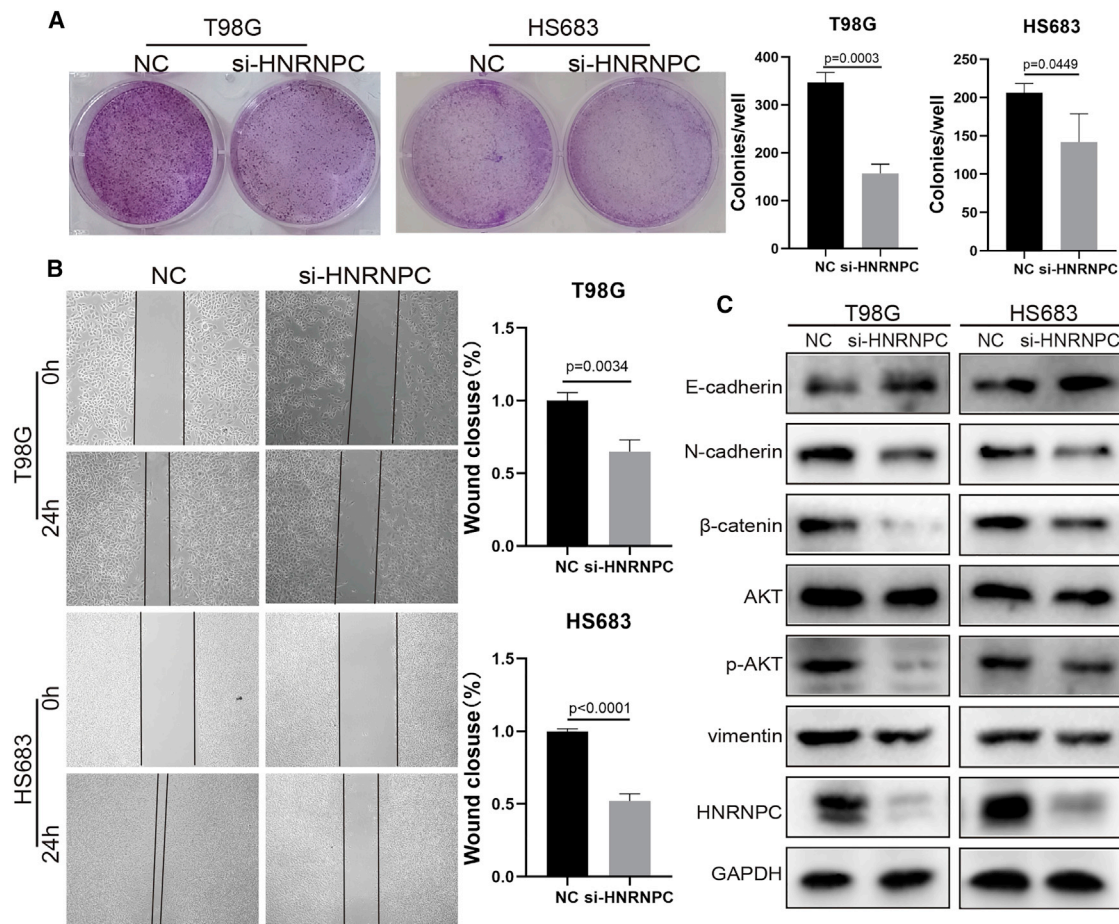


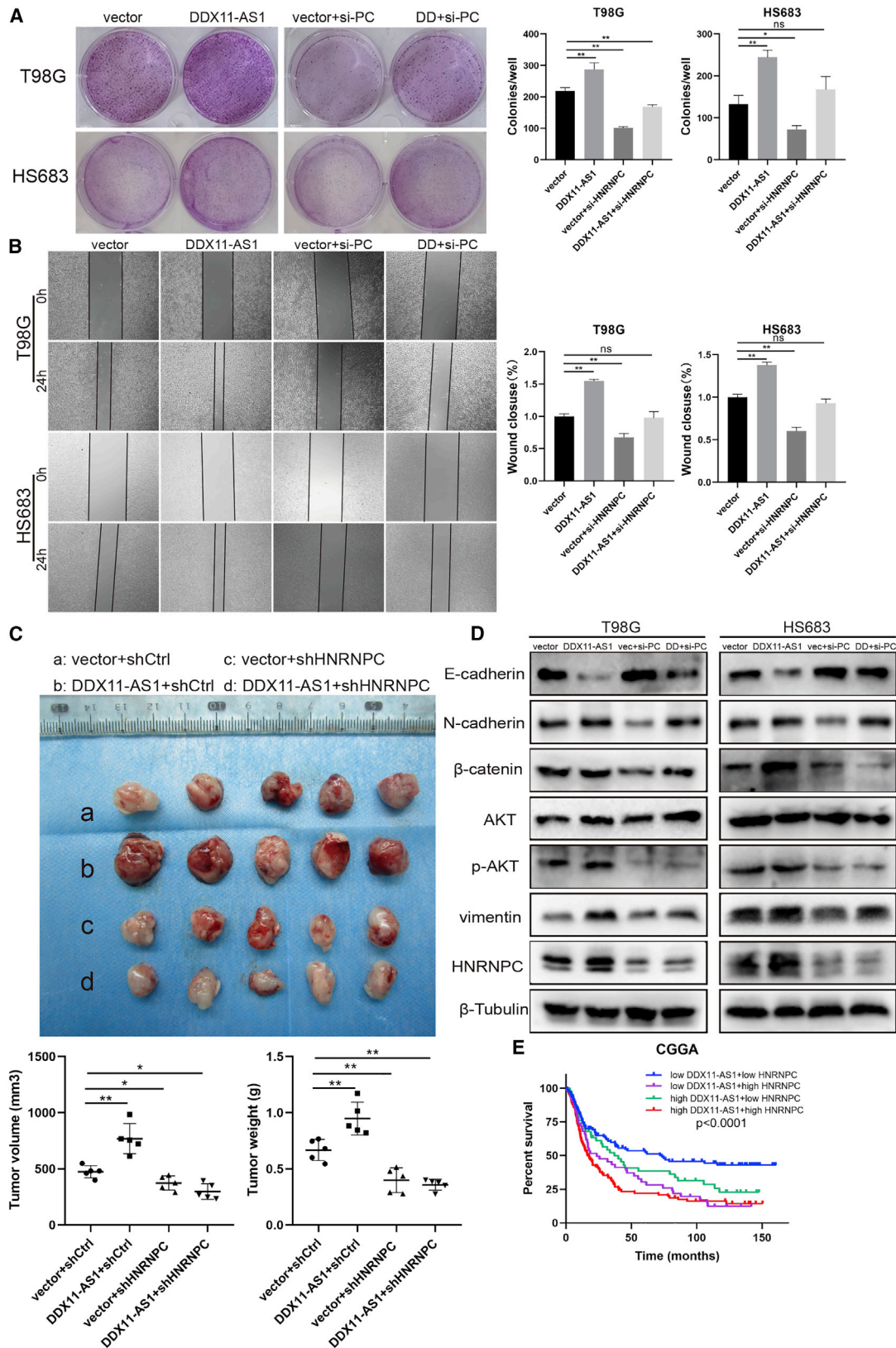
Figure 5. The effect of HNRNPC knockdown on glioma cells

(A) The clone-formation assay of HNRNPC knockdown. (B) The wound-healing assay of HNRNPC knockdown. (C) The western-blot assay of HNRNPC knockdown on the Wnt/ β -catenin and AKT pathways and EMT processes. Results represent means \pm SEM. $n = 3$. $p < 0.05$ was considered statistically significant.

Interestingly, many researchers have recently found that the interaction between lncRNAs and RBPs plays a key role in tumor progression,³⁰ and most lncRNAs can interact with one or more RBPs.³¹ Here, we first predicted the potential protein targets of DDX11-AS1 using the starBase v.2.0 website and then detected the proteins bound by DDX11-AS1 in glioma cells by CHIRP-MS. Through a comprehensive analysis, HNRNPC was selected as the potential binding target of DDX11-AS1. HNRNPC belongs to the subfamily of ubiquitously expressed heterogeneous nuclear ribonucleoproteins (hnRNPs), and the hnRNPs are RBPs.³² Many studies have shown that HNRNPC mainly acts as a regulator of m6A RNA methylation in tumors.^{32–34} Currently, HNRNPC has been reported to promote the progress of oral squamous cell carcinoma through EMT, and interaction with KH-type splicing regulatory protein induces invasion and metastasis of human lung cancer cells through activation of interferon (IFN)- α -JAK-STAT1 signaling pathway.^{33,35} Moreover, Wang et al. find that HNRNPC expression is associated with malignant glioma development, and Park et al. show that HNRNPC controls GBM cell inva-

sions by regulating PDCD4.^{34,36} In our study, the RIP experiment confirmed that HNRNPC protein binds the DDX11-AS1 molecule. Furthermore, DDX11-AS1 positively regulates the expression of HNRNPC. More importantly, the promoting effect of DDX11-AS1 on glioma was recovered by HNRNPC knockdown *in vivo* and *in vitro*. Overall, we found that DDX11-AS1 interaction with HNRNPC activated the Wnt/ β -catenin and AKT pathways and EMT processes to enhance glioma cell proliferation and migration.

In summary, our study identifies a novel mechanism of DDX11-AS1 in glioma. Our data suggest that DDX11-AS1 is up-regulated in glioma tissue and is associated with poor prognoses in glioma patients. On the mechanism, the combination of DDX11-AS1 and HNRNPC enhances Wnt/ β -catenin and AKT pathways and EMT to promote the proliferation and migration of glioma cells. The discovery of the DDX11-AS1/HNRNPC axis is expected to provide a new idea for the diagnosis and prognosis of glioma.



(legend on next page)

MATERIALS AND METHODS

Clinical samples and cell culture

In this study, 26 normal samples and 88 glioma samples were obtained from patients at Jiangxi Cancer Hospital of Nanchang University. The surgically resected tissue was immediately frozen in liquid nitrogen and stored at -80°C for subsequent RNA extraction. The study was approved by the ethics committee of Jiangxi Cancer Hospital of Nanchang University (no. 2019ky027). Informed consent was obtained from all patients. Human glioma cells T98G and HS683 were purchased from the American Type Culture Collection. The cell-growth conditions were the same as the previous method.³⁷

Cell transfection

Anti-sense oligonucleotide (ASO) that specifically target DDX11-AS1 knockdown and siRNA that specifically targets HNRNPC knockdown were purchased from RiboBio (Guangzhou, China). According to the instructions, ASO and siRNA transfection were also performed using the transfection kit from RiboBio (Guangzhou, China). The ASO targeting sequence is as follows: GGAGAATGAATT CATGCTAA; si-HNRNPC-1: CTCGAAACGTCAGCGTGTA; si-HNRNPC-2: GCCTTCGTTTCAGTATGTTA; si-HNRNPC-3: GTGAA GAAAGATGAGACTA. ASO and siRNA were transfected at 50 nM. The HNRNPC knockdown lentivirus was purchased from GenePharma (Shanghai, China), and its sequence was GCGCTTGCTAA GATCAAATT.

To construct the cell model of DDX11-AS1 overexpression, DDX11-AS1 overexpressed lentivirus was purchased from GeneChem (Shanghai, China). The DDX11-AS1 lentiviral vector was GV502. According to the instructions, 48 h after the virus concentration gradient infected the cells, the infection efficiency was observed with a fluorescence microscope. When a multiplicity of infection (MOI) was 5 with 5 $\mu\text{g}/\text{mL}$ Polybrene, the efficiency of infection can reach 80%.

Quantitative real-time PCR

The total RNA of tissue samples and cells was extracted using TRIzol reagent (Invitrogen, Carlsbad, CA, USA), and the RNA samples were stored at -80°C . The Thermo Scientific Revertaid First Strand cDNA Synthesis Kit (Thermo Fisher Scientific, Wilmington, DE, USA) was then used to reverse transcribe RNA into the First Strand cDNA. Then, according to the manufacturer's instructions, the SYBR Green Real-time PCR kit (Takara, Dalian, China) was used to perform quantitative real-time PCR. Each group was provided with three parallel holes. GAPDH was used as the Ctrl for quantitative DDX11-AS1 expression. The qPCR primer sequences were listed as follows:

DDX11-AS1 forward 5'-CCTCTGCCTACAATACAAAAGTCA-3' and reverse 5'-CAGGGTAAATGTACTTCAGCCAC-3'; GAPDH forward 5'-TGACTTCAACAGCGACACCCA-3' and reverse 5'-CACC CTGTTGCTGTAGCCAAA-3'.

Western-blot analysis

Western blot was performed as previously described.³⁷ The primary antibodies used in this study were as follows: E-cadherin, 1:2,000, Servicebio (Wuhan, China); N-cadherin, 1:2,000, Servicebio (Wuhan, China); vimentin, 1:5,000, Santa Cruz Biotechnology (Dallas, TX, USA); phospho-AKT(ser473), 1:2,000, Absin (Shanghai, China); AKT, 1:2,000, Absin (Shanghai, China); GAPDH, 1:5,000, Servicebio (Wuhan, China); β -tubulin, 1:5,000, Abmart (Shanghai, China); β -catenin, 1:2,000, Servicebio (Wuhan, China); and HNRNPC, 1:2,000, Servicebio (Wuhan, China).

Cell-proliferation and migration assays

Cell proliferation was assessed using MTT and clone -formation assays. The MTT assay involved incubating the cells in a 96-well plate with MTT reagent at the same time point for 4 consecutive days and then dissolving the blue-purple complex formed with a solvent. The absorbance of the solution was measured. The clone-formation assay was used to plant the knockdown or overexpressed DDX11-AS1 cells and the Ctrl group in a 6-well plate with 1,000 cells/well and then to stain them after the clusters containing more than 50 cells were seen under the microscope. Cell proliferation was assessed using transwell and wound-healing assays. The assays were carried out as described previously.³⁷

Flow-cytometry apoptosis assay

Annexin V-PE/7AAD double staining was used to evaluate the cell apoptotic ability. Logarithmically grown DDX11-AS1 knockdown and Ctrl cells were collected according to the PE Annexin V Apoptosis Detection Kit instruction (BD Biosciences, Franklin Lakes, NJ, USA). One-hundred μL $1 \times$ binding buffer containing 1×10^5 cells was added with 5 μL Annexin V-PE and 5 μL 7-AAD for incubation at room temperature for 15 min. Then, the Flow Cytometer (BD Accuri C6; BD Biosciences) was used within 1 h after adding 400 μL buffer solution. The data were analyzed by FlowJo software.

Animal experiment

The specific-pathogen-free (SPF) female nude mice (15–18 g, 4 weeks) were purchased from the Department of Experimental Animals, Central South University. After the nude mice adapted to the environment, logarithmically grown lentivirus-treated HS683 cells were collected for subcutaneous tumor formation in the right limb axillary

Figure 6. HNRNPC knockdown restored the induction of DDX11-AS1 overexpression

(A) The cloning-formation assays showed that HNRNPC knockdown decreased DDX11-AS1-promoted proliferation. (B) The wound-healing assay showed that HNRNPC knockdown reduced DDX11-AS1-induced migration. (C) *In vivo* experiments showed that HNRNPC knockdown inhibited the growth-promoting effect of DDX11-AS1 on glioma. $n = 5$. * $p < 0.05$, ** $p < 0.01$. (D) HNRNPC knockdown reversed the activation of DDX11-AS1 on the Wnt/ β -catenin and AKT pathways and EMT processes. (E) The overall-survival analysis of DDX11-AS1 and HNRNPC expression in the CGGA database. Results represent means \pm SEM. $p < 0.05$ was considered statistically significant. The DDX11-AS1/HNRNPC axis affects the proliferation and migration of glioma cells and activates the Wnt/ β -catenin and AKT pathways and EMT process, which provides a new idea and therapeutic target for the diagnosis, treatment, and prognosis of glioma.

region. Each nude mouse was treated with 2×10^6 cells/100 μ L PBS. By measuring the maximum length (L) and minimum length (W) and weight of the tumor, the tumor volume was calculated as $1/2 LW^2$. When the maximum volume reached 1,000 mm³, the mice were euthanized. The animal experiment was approved by the Experimental Animal Welfare Ethics Committee of Central South University.

IHC assay

Animal tumor samples were fixed with 4% paraformaldehyde and embedded in paraffin. After paraffin-embedded sections were dewaxed and dehydrated, the tissue sections were placed in a repair box filled with citric acid antigen repair buffer (PH6.0) for antigen repair. The tissue sections were then placed in a 3% hydrogen-peroxide solution to block endogenous peroxidase, closed at room temperature with 3% BSA for 30 min, and incubated overnight with Ki67 and β -catenin primary antibody (1:500; Servicebio, Wuhan, China) at 4°C. After 1 h incubation with the corresponding secondary antibody at room temperature, diaminobenzidine chromogen (DAB) solution was used for nuclear restaining. The slices were then treated with hematoxylin, dehydrated, permeated, and sealed.

CHIRP-MS

CHIRP-MS was performed by aksomics (Shanghai, China). T98G cells (2×10^8) were collected and resuspended with 1 mL precooled PBS. Formaldehyde solution (37%) was added to the cell suspension for cross-linking for 30 min at room temperature, then glycine was added to 125 mM for reaction termination. The solution was centrifuged, and the supernatant was removed to obtain a precipitate. The precipitate was dissolved in the lysis buffer by ultrasound in an ice bath for 30 min until completely dissolved, and the sample solution was obtained by centrifuging. Biotin-labeled probes were bound to magnetic beads for 30 min and then hybridized with samples overnight at 37°C. The magnetic beads were washed with 1 mL wash buffer, Benzonase (20 U) was added to react, and then they were reacted at 95°C for 30 min to remove cross-linking. Then, 0.1% SDC and 10% TCA were added and precipitated at 4°C for 2h, followed by trypsin hydrolysis, polypeptide desalination, and liquid chromatography-tandem mass spectrometry (LC-MS/MS) analysis.^{38–40}

RIP

The EZ-Magna RIP Kit (Millipore, Burlington, MA, USA) was used in the RIP experiment. According to the manufacturer's instructions, 4.0×10^7 T98G cells were collected, and cell lysates were extracted using RIP lysis buffer. The beads were then incubated with a 5 μ g HNRNPC antibody (ZEN-BIOSCIENCE, Chengdu, China) and rabbit IgG antibody. Next, cell lysates and magnetic beads were incubated overnight in the RIP immunoprecipitation buffer at 4°C. Protease K was used to digest the proteins on the magnetic beads, and the TRizol reagent was used to extract RNA from the proteins. The expression of DDX11-AS1 was evaluated by the quantitative real-time PCR method described above. The U1 snRNA in the kit was the Ctrl.

Bioinformatics analysis

RNA sequencing data of LGG and GBM samples from the TCGA were analyzed. The GEPIA analysis website⁴¹ (<http://gepia2.cancer-pku.cn/#index>) visualized the expression and correlation, with the patient survival prognosis of DDX11-AS1 and HNRNPC in LGG and GBM in the TCGA database. RNA sequencing expression data of the GSE4290 dataset containing 23 non-tumor samples and 157 glioma tumors were downloaded from the GEO database⁴² (<https://www.ncbi.nlm.nih.gov/geo/>), and the relationship between DDX11-AS1 expression and clinical information was performed in the mRNaseq_325 dataset of CGGA database⁴³ (<http://www.cgga.org.cn/index.jsp>). StarBase v.2.0 (<http://starbase.sysu.edu.cn/>) was used to analyze the RBPs of DDX11-AS1 interactions.⁴⁴

Statistical analysis

GraphPad Prism 8 was used for data statistical analysis. The two-tailed Student's t test was used for analysis between two groups. One-way ANOVA was used for multiple groups analysis. The Pearson correlation analysis method was used to analyze the correlation between DDX11-AS1 and HNRNPC. $p < 0.05$ was considered statistically significant.

SUPPLEMENTAL INFORMATION

Supplemental information can be found online at <https://doi.org/10.1016/j.omtn.2022.04.016>.

ACKNOWLEDGMENTS

We sincerely acknowledge the contributions from the TCGA, CGGA, and GSE4290 projects. This work was supported by the National Natural Science Foundation of China (no. 81860664) and the Distinguished Young Scholars Fund of Jiangxi Cancer Hospital (2021DYS01).

AUTHOR CONTRIBUTIONS

Z.X., Q.L., and X.P. conceived and designed the experiments. Z.X. conducted the experiments, analyzed the data, and wrote the original draft. Q.L., Y.Z., and X.C. did some experimental work. R.G. and S.L. directed the *in vitro/in vivo* experiments. X.P. was responsible for the revision of the manuscript. All authors read and approved the final manuscript.

DECLARATIONS OF INTERESTS

The authors have declared that no competing interest exists.

REFERENCES

1. Lenting, K., Verhaak, R., Ter Laan, M., Wesseling, P., and Leenders, W. (2017). Glioma: experimental models and reality. *Acta Neuropathol.* 133, 263–282. <https://doi.org/10.1007/s00401-017-1671-4>.
2. Bush, N.A.O., Chang, S.M., and Berger, M.S. (2017). Current and future strategies for treatment of glioma. *Neurosurg. Rev.* 40, 1–14. <https://doi.org/10.1007/s10143-016-0709-8>.
3. Louis, D.N., Ohgaki, H., Wiestler, O.D., Cavenee, W.K., Burger, P.C., Jouvett, A., Scheithauer, B.W., and Kleihues, P. (2007). The 2007 WHO classification of tumours of the central nervous system. *Acta Neuropathol.* 114, 97–109. <https://doi.org/10.1007/s00401-007-0243-4>.

4. Furnari, F.B., Fenton, T., Bachoo, R.M., Mukasa, A., Stommel, J.M., Stegh, A., Hahn, W.C., Ligon, K.L., Louis, D.N., Brennan, C., et al. (2007). Malignant astrocytic glioma: genetics, biology, and paths to treatment. *Genes Dev.* 21, 2683–2710. <https://doi.org/10.1101/gad.1596707>.
5. Sahu, A., Singhal, U., and Chinnaiyan, A.M. (2015). Long noncoding RNAs in cancer: from function to translation. *Trends Cancer* 1, 93–109. <https://doi.org/10.1016/j.trecan.2015.08.010>.
6. Huarte, M. (2015). The emerging role of lncRNAs in cancer. *Nat. Med.* 21, 1253–1261. <https://doi.org/10.1038/nm.3981>.
7. Wang, Y., Wang, Y., Li, J., Zhang, Y., Yin, H., and Han, B. (2015). CRNDE, a long-noncoding RNA, promotes glioma cell growth and invasion through mTOR signaling. *Cancer Lett.* 367, 122–128. <https://doi.org/10.1016/j.canlet.2015.03.027>.
8. Zheng, J., Liu, X., Wang, P., Xue, Y., Ma, J., Qu, C., and Liu, Y. (2016). CRNDE promotes malignant progression of glioma by attenuating miR-384/PIWIL4/STAT3 Axis. *Mol. Ther.* 24, 1199–1215. <https://doi.org/10.1038/mt.2016.71>.
9. Chen, Q., Cai, J., Wang, Q., Wang, Y., Liu, M., Yang, J., Zhou, J., Kang, C., Li, M., and Jiang, C. (2018). Long noncoding RNA NEAT1, regulated by the EGFR pathway, contributes to glioblastoma progression through the WNT/ β -Catenin pathway by scaffolding EZH2. *Clin. Cancer Res.* 24, 684–695. <https://doi.org/10.1158/1078-0432.Ccr-17-0605>.
10. Bi, C.L., Liu, J.F., Zhang, M.Y., Lan, S., Yang, Z.Y., and Fang, J.S. (2020). LncRNA NEAT1 promotes malignant phenotypes and TMZ resistance in glioblastoma stem cells by regulating let-7g-5p/MAP3K1 axis. *Biosci. Rep.* 40, BSR20201111. <https://doi.org/10.1042/bsr20201111>.
11. Chen, D., Chen, J., Gao, J., Zhang, Y., Ma, Y., Wei, W., and Wei, Y. (2020). LncRNA DDX11-AS1 promotes bladder cancer occurrence via protecting LAMB3 from down-regulation by sponging miR-2355-5p. *Cancer Biother. Radiopharm.* 35, 319–328. <https://doi.org/10.1089/cbr.2019.3021>.
12. Feng, X., Yang, S., Zhou, S., Deng, S., and Xie, Y. (2020). Long non-coding RNA DDX11-AS1 promotes non-small cell lung cancer development via regulating PI3K/AKT signalling. *Clin. Exp. Pharmacol. Physiol.* 47, 1622–1631. <https://doi.org/10.1111/1440-1681.13325>.
13. Feng, Y., Wu, M., Hu, S., Peng, X., and Chen, F. (2020). LncRNA DDX11-AS1: a novel oncogene in human cancer. *Hum. Cell* 33, 946–953. <https://doi.org/10.1007/s13577-020-00409-8>.
14. Li, Q., Wang, S., Wu, Z., and Liu, Y. (2020). DDX11-AS1 exacerbates bladder cancer progression by enhancing CDK6 expression via suppressing miR-499b-5p. *Biomed. Pharmacother.* 127, 110164. <https://doi.org/10.1016/j.biopha.2020.110164>.
15. Ren, Z., Liu, X., Si, Y., and Yang, D. (2020). Long non-coding RNA DDX11-AS1 facilitates gastric cancer progression by regulating miR-873-5p/SPC18 axis. *Artif. Cells Nanomed Biotechnol.* 48, 572–583. <https://doi.org/10.1080/21691401.2020.1726937>.
16. Song, W., Qian, Y., Zhang, M.H., Wang, H., Wen, X., Yang, X.Z., and Dai, W.J. (2020). The long non-coding RNA DDX11-AS1 facilitates cell progression and oxaliplatin resistance via regulating miR-326/IRS1 axis in gastric cancer. *Eur. Rev. Med. Pharmacol. Sci.* 24, 3049–3061. https://doi.org/10.26355/eurrev_202003_20669.
17. Ding, G., Zeng, Y., Yang, D., Zhang, C., Mao, C., Xiao, E., Kang, Y., and Shang, J. (2021). Silenced lncRNA DDX11-AS1 or up-regulated microRNA-34a-3p inhibits malignant phenotypes of hepatocellular carcinoma cells via suppression of TRAF5. *Cancer Cell Int.* 21, 179. <https://doi.org/10.1186/s12935-021-01847-6>.
18. Wu, C., Wang, Z., Tian, X., Wang, J., Zhang, Y., and Wu, B. (2021). Long non-coding RNA DDX11-AS1 promotes esophageal carcinoma cell proliferation and migration through regulating the miR-514b-3p/RBX1 axis. *Bioengineered* 12, 3772–3786. <https://doi.org/10.1080/21655979.2021.1940617>.
19. Xu, M., Zhao, X., Zhao, S., Yang, Z., Yuan, W., Han, H., Zhang, B., Zhou, L., Zheng, S., and Li, M.D. (2021). Landscape analysis of lncRNAs shows that DDX11-AS1 promotes cell-cycle progression in liver cancer through the PARP1/p53 axis. *Cancer Lett.* 520, 282–294. <https://doi.org/10.1016/j.canlet.2021.08.001>.
20. Craene, B.D., and Bex, G. (2013). Regulatory networks defining EMT during cancer initiation and progression. *Nat. Rev. Cancer* 13, 97–110. <https://doi.org/10.1038/nrc3447>.
21. Kahlert, U.D., Nikkiah, G., and Maciaczyk, J. (2013). Epithelial-to-mesenchymal(-like) transition as a relevant molecular event in malignant gliomas. *Cancer Lett.* 331, 131–138. <https://doi.org/10.1016/j.canlet.2012.12.010>.
22. Samatov, T.R., Tonevitsky, A.G., and Schumacher, U. (2013). Epithelial-mesenchymal transition: focus on metastatic cascade, alternative splicing, non-coding RNAs and modulating compounds. *Mol. Cancer* 12, 107. <https://doi.org/10.1186/1476-4598-12-107>.
23. Zhang, K., Zhang, J., Han, L., Pu, P., and Kang, C. (2012). Wnt/ β -catenin signaling in glioma. *J. Neuroimmune Pharmacol.* 7, 740–749. <https://doi.org/10.1007/s11481-012-9359-y>.
24. Chautard, E., Ouédraogo, Z.G., Biau, J., and Verrelle, P. (2014). Role of Akt in human malignant glioma: from oncogenesis to tumor aggressiveness. *J. Neurooncol.* 117, 205–215. <https://doi.org/10.1007/s11060-014-1382-9>.
25. Zheng, Y., Xie, J., Xu, X., Yang, X., Zou, Y., Yao, Q., and Xiong, Y. (2021). LncRNA DDX11-AS1 exerts oncogenic roles in glioma through regulating miR-499b-5p/RWDD4 Axis. *Onco Targets Ther.* 14, 157–164. <https://doi.org/10.2147/ott.S278986>.
26. Zhang, Y., Huang, W., Yuan, Y., Li, J., Wu, J., Yu, J., He, Y., Wei, Z., and Zhang, C. (2020). Long non-coding RNA H19 promotes colorectal cancer metastasis via binding to hnRNP A2B1. *J. Exp. Clin. Cancer Res.* 39, 141. <https://doi.org/10.1186/s13046-020-01619-6>.
27. He, X., Sheng, J., Yu, W., Wang, K., Zhu, S., and Liu, Q. (2021). LncRNA MIR155HG promotes temozolomide resistance by activating the Wnt/ β -catenin pathway via binding to PTBP1 in glioma. *Cell Mol. Neurobiol.* 41, 1271–1284. <https://doi.org/10.1007/s10571-020-00898-z>.
28. Ponting, C.P., Oliver, P.L., and Reik, W. (2009). Evolution and functions of long non-coding RNAs. *Cell* 136, 629–641. <https://doi.org/10.1016/j.cell.2009.02.006>.
29. Hu, X., Sood, A.K., Dang, C.V., and Zhang, L. (2018). The role of long noncoding RNAs in cancer: the dark matter matters. *Curr. Opin. Genet. Dev.* 48, 8–15. <https://doi.org/10.1016/j.gde.2017.10.004>.
30. Yao, Z.T., Yang, Y.M., Sun, M.M., He, Y., Liao, L., Chen, K.S., and Li, B. (2022). New insights into the interplay between long non-coding RNAs and RNA-binding proteins in cancer. *Cancer Commun.* 42, 117–140. <https://doi.org/10.1002/cac2.12254>.
31. Ferrè, F., Colantoni, A., and Helmer-Citterich, M. (2016). Revealing protein-lncRNA interaction. *Brief. Bioinformatics* 17, 106–116. <https://doi.org/10.1093/bib/bbv031>.
32. Bi, Z., Liu, Y., Zhao, Y., Yao, Y., Wu, R., Liu, Q., Wang, Y., and Wang, X. (2019). A dynamic reversible RNA N(6)-methyladenosine modification: current status and perspectives. *J. Cell. Physiol.* 234, 7948–7956. <https://doi.org/10.1002/jcp.28014>.
33. Huang, G.Z., Wu, Q.Q., Zheng, Z.N., Shao, T.R., Chen, Y.C., Zeng, W.S., and Lv, X.Z. (2020). M6A-related bioinformatics analysis reveals that HNRNPC facilitates progression of OSCC via EMT. *Aging* 12, 11667–11684. <https://doi.org/10.18632/aging.103333>.
34. Wang, L.C., Chen, S.H., Shen, X.L., Li, D.C., Liu, H.Y., Ji, Y.L., Li, M., Yu, K., Yang, H., Chen, J.J., et al. (2020). M6A RNA methylation regulator HNRNPC contributes to tumorigenesis and predicts prognosis in glioblastoma Multiforme. *Front. Oncol.* 10, 536875. <https://doi.org/10.3389/fonc.2020.536875>.
35. Yan, M., Sun, L., Li, J., Yu, H., Lin, H., Yu, T., Zhao, F., Zhu, M., Liu, L., Geng, Q., et al. (2019). RNA-binding protein KHSRP promotes tumor growth and metastasis in non-small cell lung cancer. *J. Exp. Clin. Cancer Res.* 38, 478. <https://doi.org/10.1186/s13046-019-1479-2>.
36. Park, Y.M., Hwang, S.J., Masuda, K., Choi, K.M., Jeong, M.R., Nam, D.H., Gorospe, M., and Kim, H.H. (2012). Heterogeneous nuclear ribonucleoprotein C1/C2 controls the metastatic potential of glioblastoma by regulating PDCD4. *Mol. Cell. Biol.* 32, 4237–4244. <https://doi.org/10.1128/mcb.00443-12>.
37. Xiang, Z., Lv, Q., Chen, X., Zhu, X., Liu, S., Li, D., and Peng, X. (2020). Lnc GNG12-AS1 knockdown suppresses glioma progression through the AKT/GSK-3 β / β -catenin pathway. *Biosci. Rep.* 40, BSR20201578. <https://doi.org/10.1042/bsr20201578>.
38. Chu, C., Zhang, Q.C., da Rocha, S.T., Flynn, R.A., Bharadwaj, M., Calabrese, J.M., Magnuson, T., Heard, E., and Chang, H.Y. (2015). Systematic discovery of Xist RNA binding proteins. *Cell* 161, 404–416. <https://doi.org/10.1016/j.cell.2015.03.025>.
39. McHugh, C.A., Chen, C.K., Chow, A., Surka, C.F., Tran, C., McDonel, P., Pandya-Jones, A., Blanco, M., Burghard, C., Moradian, A., et al. (2015). The Xist lncRNA interacts directly with SHARP to silence transcription through HDAC3. *Nature* 521, 232–236. <https://doi.org/10.1038/nature14443>.

40. Chai, P., Jia, R., Jia, R., Pan, H., Wang, S., Ni, H., Wang, H., Zhou, C., Shi, Y., Ge, S., et al. (2018). Dynamic chromosomal tuning of a novel GAU1 lncing driver at chr12p13.32 accelerates tumorigenesis. *Nucleic Acids Res.* *46*, 6041–6056. <https://doi.org/10.1093/nar/gky366>.
41. Tang, Z., Li, C., Kang, B., Gao, G., Li, C., and Zhang, Z. (2017). GEPIA: a web server for cancer and normal gene expression profiling and interactive analyses. *Nucleic Acids Res.* *45*, W98–W102. <https://doi.org/10.1093/nar/gkx247>.
42. Sun, L., Hui, A.M., Su, Q., Vortmeyer, A., Kotliarov, Y., Pastorino, S., Passaniti, A., Menon, J., Walling, J., Bailey, R., et al. (2006). Neuronal and glioma-derived stem cell factor induces angiogenesis within the brain. *Cancer cell* *9*, 287–300. <https://doi.org/10.1016/j.ccr.2006.03.003>.
43. Zhao, Z., Zhang, K.N., Wang, Q., Li, G., Zeng, F., Zhang, Y., Wu, F., Chai, R., Wang, Z., Zhang, C., et al. (2021). Chinese glioma genome Atlas (CGGA): a comprehensive resource with functional genomic data from Chinese glioma patients. *Genomics Proteomics Bioinformatics* *19*, 1–12. <https://doi.org/10.1016/j.gpb.2020.10.005>.
44. Li, J.H., Liu, S., Zhou, H., Qu, L.H., and Yang, J.H. (2014). starBase v2.0: decoding miRNA-ceRNA, miRNA-ncRNA and protein-RNA interaction networks from large-scale CLIP-Seq data. *Nucleic Acids Res.* *42*, D92–D97. <https://doi.org/10.1093/nar/gkt1248>.